Modeling, Developing, and Optimizing Minimal Cislunar PNT Constellations

Dillon W. Smith*

Cislunar space is expected to see a large increase in number of users over the next few decades. As a result, a cislunar positioning, navigation, and timing (PNT) service should be implemented in order to meet the demanding needs of users. Focus is placed on a near term version of the system that will cater to areas of interest in cislunar space, namely the lunar south pole. A standard set of metrics, including coverage and Positional Dilution of Precision (PDOP), are utilized to assess and compare various system configurations proposed in literature. Architectural changes are imposed onto literature constellations to produce novel constellations with the goal of increasing performance, which is achieved. To systematically improve constellation performance, an optimization process to determine the optimal satellite positioning along defined orbits is used to minimize PNT estimate errors. Optimized constellations are developed and compared to the originals in which it is seen that major performance increases are possible.

I. Nomenclature

DOP	=	Dilution of Precision
$EFLO$	=	Elliptical Frozen Lunar Orbit
$GDOP$	=	Geometric Dilution of Precision
$GNSS$	=	Global Navigation Satellite System
$GMAT$	=	General Mission Analysis Tool
GPS	=	Global Positioning System
IMU	=	Internal Measurement Unit
LSP	=	Lunar South Pole
$NRHO$	=	Near Rectilinear Halo Orbit
$PDOP$	=	Positional Dilution of Precision
PNT	=	Positioning, Navigation, and Timing
$TDOP$	=	Time Dilution of Precision
UNE	=	User Navigation Error
$UERE$	=	User Equivalent Range Error

II. Introduction

Cislunar space is a region garnering a large increase of interest for planned space missions as the moon is seen as a gateway to the rest of the solar system. The surface can potentially serve as a resource for extended missions, and special orbits in cislunar space can act as a staging environment for refueling rendezvous. An essential aspect of a space mission is being able to obtain accurate positioning, navigation, and timing (PNT) estimates to determine user location and navigation solutions. Making a PNT estimate involves receiving signals from a source with highly accurate knowledge of its own location to in turn calculate a position fix. Currently, cislunar space relies heavily on the use of the DSN and other Earth based systems for PNT needs; however, as the number of users within cislunar space increases along with PNT requirements, Earth based systems cannot meet rising demands .

A solution to this problem is the introduction of a dedicated cislunar PNT infrastructure. Such a system has been proposed in different pieces of literature through recent years, but focus largely appears to be directed at final phase solutions while neglecting near term implementations. Creating an optimal and fully implemented solution will be imperative for the future, but it will take decades to properly implement and will likely follow an iterative process similar to those utilized when implementing the GNSS and GPS constellations. Meanwhile, users operating in cislunar space

*Georgia Institute of Technology

throughout the current decade will still require PNT services. Therefore, careful consideration should be placed on early stage minimal satellite configurations of a dedicated PNT system that will meet the needs of near term users while being easily scalable into a full scale late stage architecture.

III. Motivation

The DSN has proven to be a reliable state of the art for providing PNT services to a majority of space missions. The system consists of a network of Earth based satellite facilities spread around the globe, with its three major locations spaced out approximately 120 degrees longitudinally in order to allow any deep space satellite to have constant communication capabilities. Common methods that the DSN utilizes to provide PNT information includes Doppler tracking, in which the relative motion of the transmitter and receiver causes a shift in frequency that indicates range rate [1], and delta differential one-way ranging, in which angular information regarding a target is obtained by measuring the direction of its incoming frequencies in comparison to radio waves from a positionally well known universal reference [2]. Despite these methods working well, the DSN should no longer be explicitly relied upon for cislunar PNT as it is quickly becoming overcrowded. With the increase in spacecraft over the past decade, the limited bandwidth of the DSN has become stretched thin. For the users relying on the DSN, this means that PNT fixes are becoming less frequent and for shorter time periods. With this, it is not recommended that the DSN be completely replaced; instead, it is recommended that a dedicated PNT service for cislunar space be implemented in order to transition the DSN into an auxiliary role.

Another PNT solution that has been proposed for cislunar space is the use of weak GNSS signals. GNSS architectures emit low power signals at specified frequencies that can be received in order to allow a user to obtain a positioning solution. Nominally, navigation by means of GNSS utilizes trilateration, which is a method to pinpoint a location in 3D space by receiving pseudorange measurements from at least four satellites. Given the vast array of GNSS satellites already in orbit, it would be beneficial to incorporate them into a cislunar PNT architecture. However, the primary use for GNSS systems are for Earth based navigation, meaning that these systems emit signals downwards towards the Earth. Despite this, it has been shown that a portion of the emitted signals escape around the Earth and reach cislunar space. With highly accurate clocks, cislunar satellites have been shown to utilize these signals to obtain a position fix with only tens of meters of uncertainty [3]. This is promising, but it is important to keep in mind that GNSS signals are weak in nature, and collecting them in cislunar space requires high gain receivers, which places a constraint on the user. With satellites adopting a smaller form factor, allocating mass and volume has become increasingly critical in which high gain antennas may not be an option.

In the long term, it is important to consider the needs of users when developing a cislunar PNT solution. In a NASA report, key findings regarding the expected performance requirements of users are presented [4]. Selected key positioning requirements from the study are displayed in Table 1.

Use Case	Positioning Error (3σ)
Surface Operations	30 m
Precision Landings	100 m
Surface Rendezvous	10 m
Ascent	10 m
Constellations	100 m
Formation Flying	10 m - 3 cm

Table 1   Expected 3-sigma positioning requirements for different cislunar operational cases [4]

As can be seen, positioning requirements range from 3 cm to 100 m depending on the use case. To support a user requiring more stringent positioning requirements, utilizing only the DSN and weak GNSS will not suffice, which further emphasizes the need for a dedicated cislunar PNT system. It is important to note however, that cases requiring extremely precise PNT solutions, such as formation flying, may not be able to be supported by a cislunar PNT system until a later stage of its implementation. A late stage phase of a PNT system is characterized by having a large number of dedicated PNT satellites along with a network of supporting ground nodes. Other operations, such as surface operations, precision landings, and surface rendezvous, have target requirements that have the potential to be met by an early stage

system. An early stage phase is characterized by only containing four to eight dedicated PNT satellites in a couple of optimal orbits. Of specific interest are ground use cases, which are targeted to be carried out in the near future. Therefore, it is important to first focus on developing a cislunar PNT architecture consisting of minimal satellites that will excel in providing PNT solutions to surface users. This is corroborated by the expressed interest in exploring the lunar south pole, thus making it the primary target of this work.

IV. Metrics of Interest

In order to compare proposed constellations of an early stage cislunar PNT system, standard metrics must be introduced. Determining these metrics will allow for an equitable comparison to be carried out. Some metrics are explored in the current work, and others need to be implemented in the future to allow for a comprehensive study.

A. System Coverage

Coverage refers to the amount of time that a user has access to the PNT system. For this study, a user is said to have access to the system when it is in view of at least four PNT satellite. Furthermore, a satellite is in view of a target when there is a clear line of sight between the satellite and the user, and if the satellite has an angle with the local horizon of at least 5 degrees. The inclusion of the 5 degree constraint takes into account the varying geography of the lunar surface to ensure general satellite visibility. Along with coverage, the average number of satellites in view for locations of interest will be kept as a comparison metric. Even though only four satellites are required to be in view to obtain a PNT solution, a greater number of satellites allows for a better PNT estimate.
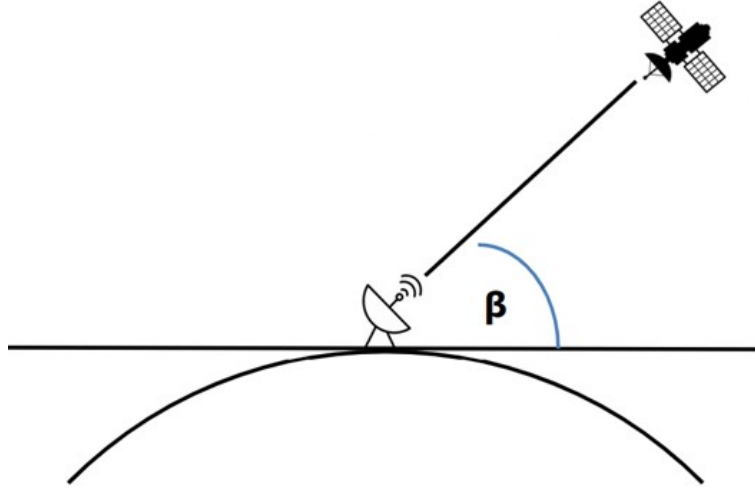

Fig. 1   Visibility requirements with $\beta \geq 5°$

B. Gap Time

Gap time refers to the amount of time that a user does not have access to the PNT system. Therefore, it is defined as when there are fewer than four satellites in view of a target user, and it will be calculated as the difference between the total propagation time and the total amount of time that coverage is available.

$$T_{gap} = T_{prop} - T_{cov} \tag{1}$$

A variant of gap time that may prove to be more insightful is instead calculating the maximum continuous gap time that a user will experience. This is because many users will possess Inertial Measurement Units (IMUs) independent of the PNT system that they will rely on during the absence of coverage. In turn, users will maintain a position estimate during gap periods that will become increasingly worse the longer the gap time. Therefore, frequent periods of smaller gaps may be preferable to fewer periods of larger gaps.

C. Positional Dilution of Precision

Positional Dilution of Precision (PDOP) refers to the uncertainty introduced into a position measurement due to the geometry of the system. Ideally, PDOP for a given constellation should be as small as possible to maintain higher accuracy PNT measurements, and this occurs when the PNT satellite geometry is the most diverse. The reasoning for
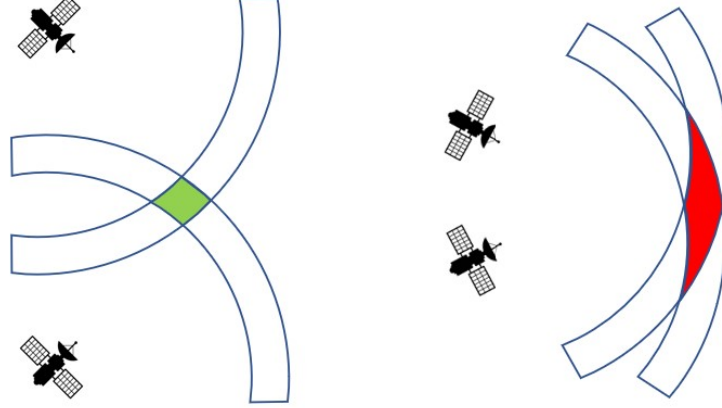

Fig. 2   The affect of PNT satellite geometry on measurement uncertainty

this is that each pseudorange measurement from a PNT satellite contains uncertainty, which creates a ring-like area surrounding the PNT satellite that contains the true location of the target user. When the angle between the satellites as referenced from the target is smaller, there is a larger portion of overlap of regions of uncertainty from individual satellites. This is visually demonstrated in Figure 2. To define PDOP as a comparison metric, this study will calculate the average PDOP over time for target users.

PDOP is only defined for a target if the user can receive at least four signals from different PNT satellites at one time. This is due to the fact that at least four range measurements are required in order to determine the position of a user in 3D space using the trilateration method. To calculate PDOP, the matrix H must first be created using position knowledge of the system.

$$H = \begin{bmatrix} \frac{x_1-x}{\|r_1\|} & \frac{y_1-y}{\|r_1\|} & \frac{y_1-y}{\|r_1\|} & -1 \\ \frac{x_2-x}{\|r_2\|} & \frac{y_2-y}{\|r_2\|} & \frac{y_2-y}{\|r_2\|} & -1 \\ & \vdots & & \\ \frac{x_n-x}{\|r_n\|} & \frac{y_n-y}{\|r_n\|} & \frac{z_n-z}{\|r_n\|} & -1 \end{bmatrix} \tag{2}$$

Here, x, y, and z denote the Cartesian coordinates of a user, while the x_1, y_1, and z_1 denote the Cartesian coordinates of one PNT satellite. The $\|r\|$ terms represent the distance between the PNT satellite and the user. It is noted that to meet the requirement of utilizing at least four range measurements, n must be ≥ 4. Using the H matrix, the Geometric Dilution of Precision (GDOP) covariance matrix can be calculated.

$$Q = (H^T H)^{-1} = \begin{bmatrix} \sigma_x^2 & \sigma_{xy} & \sigma_{xz} & \sigma_{xt} \\ \sigma_{xy} & \sigma_y^2 & \sigma_{yz} & \sigma_{yt} \\ \sigma_{xz} & \sigma_{yz} & \sigma_z^2 & \sigma_{zt} \\ \sigma_{xt} & \sigma_{yt} & \sigma_{zt} & \sigma_t^2 \end{bmatrix} \tag{3}$$

Within the covariance matrix, Q, the diagonal elements represent the variances of the x, y, and z positional uncertainties along with the time uncertainty, t. The off diagonal elements represent the covariances between terms. To extract the PDOP, the root sum is taken of the positional variances.

$$PDOP = \sqrt{\sigma_x^2 + \sigma_y^2 + \sigma_z^2} \tag{4}$$

D. User Navigation Error

User navigation error (UNE) refers to the compounded uncertainty a positional measurement carries due to geometric, systematic, and environmental sources. UNE is defined as the product of the PDOP and user equivalent range error (UERE).

$$UNE = PDOP \cdot UERE \tag{5}$$

PDOP is defined as it was previously, and UERE is the combination of environmental and system induced uncertainties. For this study, UERE will remain as a constant value that is calculated as the root sum square of the contributors shown in Table 2. These values are the worst case uncertainty contributors from the individual sources listed in the table. The values were determined using clock errors translated into positional uncertainty, average errors associated with lunar orbit determination [5], and receiver noise and multipath errors [6]. The total represents the root mean sum of the individual contributors, and will be utilized as the 3σ UERE.

Source	3σ Position Error
Clock Model	9.44 m
Orbit Uncertainty	9.53 m
Receiver Noise	20.80 m
Multipath Error	2.06 m
Total RSS	24.84 m

Table 2 3σ UERE error from major contributors

E. Station Keeping Costs

A goal for designing a cislunar PNT architecture should be that it has longevity. Similar to GNSS architectures, a cislunar system should aim to be of service for decades. To do this, orbits need to be maintained, which usually occurs by periodically exerting a small thrust. This is a simple task for Earth orbits; however, most lunar orbits are unstable due to the three body effects from the Earth and other various perturbations. With this, station keeping costs can rise considerably depending on the type of orbit. Two large categories of stable lunar orbits that are being explored are Elliptical Frozen Lunar Orbits (EFLOs) and Near Rectilinear Halo Orbits (NRHOs). EFLOs are constructed such that the drift in their orbital parameters are minimized, and analytical solutions to calculating families of EFLOs exist [7]. NRHOs are a different group of orbits that utilize the Lagrangian points within the Earth-Moon system. These unique areas of space with balancing gravitational forces allow for stable orbits to be achieved [8]. Specifically, NRHOs exhibit highly eccentric orbits that exist at the edge of Lagrangian points which allow for near lunar passes.

The calculation of station keeping costs is not performed in this study. In the future, it can be done by utilizing Lambert's problem to calculate the δv cost of transferring from a drifted orbit to the initial orbit at the point of lowest cost. This study utilizes constellations containing EFLOs and NRHOs in order to keep stationkeeping costs low without directly using it as a comparison metric. However, it is noted that not all EFLOs and NRHOs required the same minimum level of station keeping. Therefore, this metric should be incorporated into a future study.

V. Modeling Process

In order to calculate the metrics of interest for different cislunar constellations, a comprehensive modeling process was developed. To ensure ease of use, most portions of the process were designed in order to require minimal manual input. The major steps of the process can be broken into three sections: inputs, propagation, and post processing.
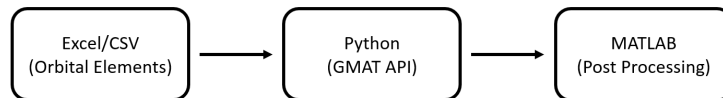

Fig. 3   Modeling flow path, with each box corresponding to major steps

A. Inputs

Six independent Keplerian orbital elements can comprehensively define the geometry of an orbit. In that sense, these six classical elements are used as inputs to the modeling process to define the cislunar PNT constellation. An input into the modeling process takes the form of a .csv file, in which there are seven columns and as many rows as necessary. The first column contains a number that identifies which specific satellite in a constellation is represented by that row. The remaining columns define the orbital elements of that satellite in the order shown in Table 3. A single input file should contain as many satellites and constellations as desired to be propagated and processed as the tool will automatically delineate separate constellations as long as the correct format is upheld. It is noted that most minimal cislunar PNT constellations utilize a set of orbits with multiple satellites within each orbit, meaning that many satellites will share all orbital elements besides the true anomaly. True anomaly defines the location of a satellite within in orbit, which can be set to increase the average number of satellites in view to a target or to minimize PDOP. After the desired constellations are loaded into and formatted correctly in a .csv format, the file is read into Python. From here, the input file is parsed and its contents are reformatted to be utilized in the next stage of the process.

Parameter	Symbol
Semimajor Axis	a
Eccentricity	e
Inclination	i
RAAN	Ω
Argument of Periapsis	ω
True Anomaly	ν

Table 3   Classical Keplerian orbital elements

B. Propagation

Lunar orbits are much more complex and unstable in comparison to Earth orbits. The main reason for this is that the Earth has a large enough mass and is close enough to the moon that it induces a large gravitational perturbation on the satellite-moon system. In turn, this causes a significant amount of drift in most lunar orbits which for many applications, such as designing a cislunar PNT system, is seen as undesirable. Due to these perturbations, the Two Body approximation cannot be employed when modeling a lunar orbit. To handle the more complex dynamics, the General Mission Analysis Tool (GMAT) is utilized.

GMAT contains an all inclusive environment that contains advanced dynamical models in order to facilitate an accurate propagation of any space mission. It was chosen to be utilized for this study due to its ease of use with cislunar applications. For modeling lunar orbits in this study, all perturbations produced from the major bodies in the solar system were included for the most accurate simulation results. The propagation itself utilizes an eighth order Runge-Kutta temporal discretization scheme, where eighth order means that the uncertainty in each time step is of the order 10^{-8}. Furthermore, the propagation step size was set to be within 0.001 to 60 seconds. It is noted that it is desirable to enforce that a constant step size be taken during propagation in order to preserve consistency; however, occasionally, a step size would be too large and cause the propagator to throw an error as it violate accuracy constraints at the given step size. Ultimately, most constellation simulations kept a constant step size of 60 seconds for the entire

Parameter	Configuration
Discretization Method	Runge-Kutta 89
Local Truncation Error	$O(\Delta t^{-8})$
Step Size (s)	0.001 - 60
Propagation Time (s)	86400

Table 4   Propagation settings within GMAT

propagation; only constellations with strange geometries, like extremely small perilunes, would require a step size decrease. Each constellation is propagated for a period of one day.

As mentioned, the goal when developing this process was to automate it as much as possible. Therefore, to initialize the propagation, the input orbital elements that were loaded into Python are automatically written to a GMAT script file. Each constellation included in the input is separated into its own GMAT script file so that each script contains one constellation case study. Every script generated is then automatically and sequentially loaded into GMAT and ran using the GMAT Python API. Propagation outputs, which contain the complete ephemeris data of each satellite in each constellation through the entire propagation, are then automatically written to a designated folder for post processing.

C. Post Processing

The metrics of interest that define the performance of a constellation are calculated post propagation using MATLAB. It is noted that GMAT does provide a wide variety of data, such as the contact time between a satellite and ground station, that would be useful for determining metrics of interest; however, MATLAB was selected for use in order to allow for complete control about how the metrics will be calculated. With this, all post processing was completed by using the positional ephemerides produced from GMAT, which is enough information to determine the metrics listed in Section IV. To be consistent with the automation efforts made for the previous portions of the modeling process, all relevant metrics are produced from by simply loading in the GMAT output file handle of the constellation that is desired into the MATLAB post processing script. All plots produced during this process maintain a standard set of configurations in order to facilitate the comparisons between constellations.

Key outputs include orbit visualizations with the average number of satellites in view displayed as a color map on the surface of the moon, plots indicating the number of satellites in view to a ground station as a function of time, and plots of the UNE over time for the south pole. All of these outputs will be explored as they are applied to constellations. To assist with determining metrics, a grid of ground stations was created on the lunar surface, which is shown in Figure 4. The created ground stations are spread equally apart by 10 degrees latitudinally and 20 degrees longitudinally. This results in a grid of 325 ground stations.
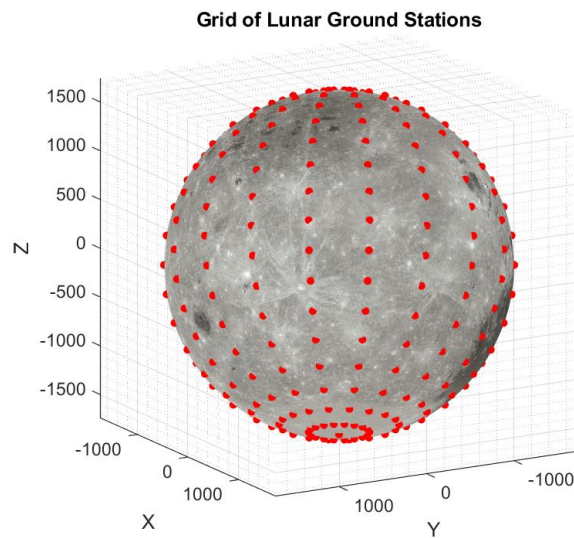

Fig. 4   Grid of ground stations spread across the lunar surface

VI. Constellations from Literature

Full scale cislunar PNT systems encompass the majority of architectures that are currently proposed in literature, with an example being one from Pereira that contains 24 PNT satellites [9]. These architectures are useful in order to simulate the performance of a future cislunar PNT service; however, it is likely that these full systems will not be operational for many years. To address the near term, some works have been published analyzing minimal architectures

on the grounds of assessing initial performances. In order to assess these architectures and to define a base, the constellations from literature will be put through the modeling process previously discussed. Two constellations will be examined: a four and eight satellite architecture.

A. Four Satellite Constellation

Four satellites is the minimum number of satellites that will be examined in an architecture for this study. This is due to the fact that for PNT by means of trilateration, which is the method used by GNSS and GPS, there must be a range measurement from at least four satellites. Less than four satellites would mean that the user would not be able to obtain a direct position fix from the PNT system. The four satellite constellation examined is derived from elements proposed by Bhamidipati Et al. [10], in which different lunar orbit types are compared for their efficacy in designing a lunar navigation system. This constellation utilizes the parameters referenced in the work, which defines an EFLO geometry that is translated into two orbital planes. The orbital elements are shown in Table 5.

Satellite	a	e	i	Ω	ω	ν_o
1	9750.5	0.70	63.50	0	90	0
2	9750.5	0.70	63.50	0	90	180
3	9750.5	0.70	63.50	180	90	0
4	9750.5	0.70	63.50	180	90	180

Table 5   Orbit defining elements for the four satellite constellation

This constellation exhibits a common characteristic that will be seen in most other constellations, which is that minimal designs of a cislunar PNT system utilize two orbits that are mirrored across the lunar poles. This is visualized in Figure 5a. The color map denotes the average number of satellites in view at all ground locations over the course of the constellation propagation. Each lunar surface panel corresponds to one of the ground stations defined by the grid shown in Figure 4., in which each panel is centered around one point grid point. By looking at Figure 5a, it can immediately been seen that the lunar south pole receives the highest coverage as it exhibits the highest average number of satellites in view. It is also noted that when examining future constellations with more than four satellites, the color map will maintain an upper limit of four satellites in order to allow for a direct comparison. Figure 5b unwraps
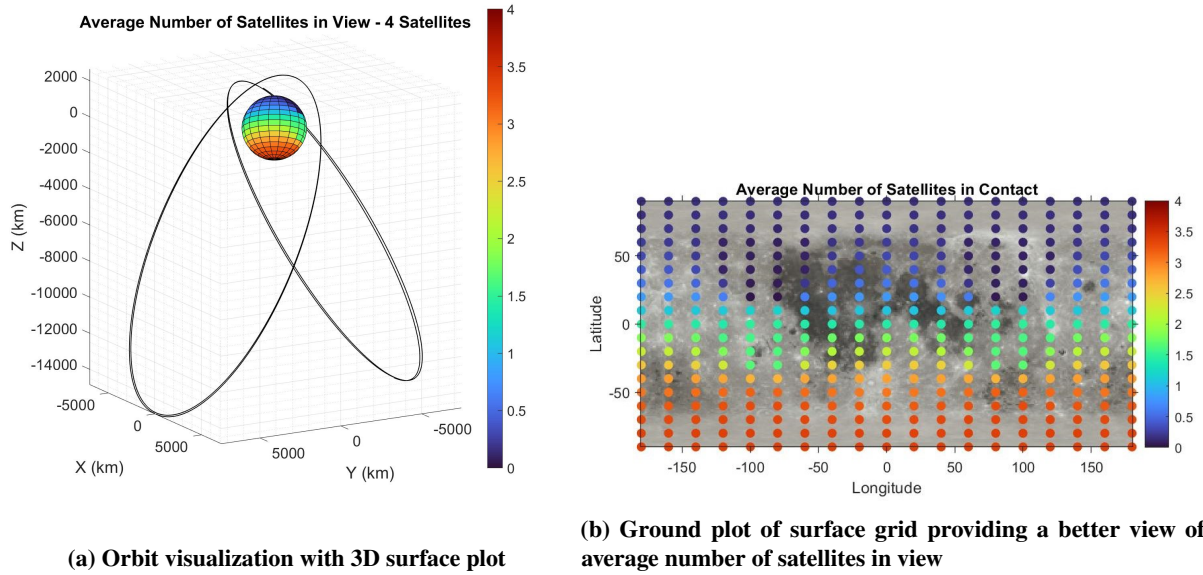

(a) Orbit visualization with 3D surface plot

(b) Ground plot of surface grid providing a better view of average number of satellites in view

Fig. 5   Global performance visualization for the four satellite constellation
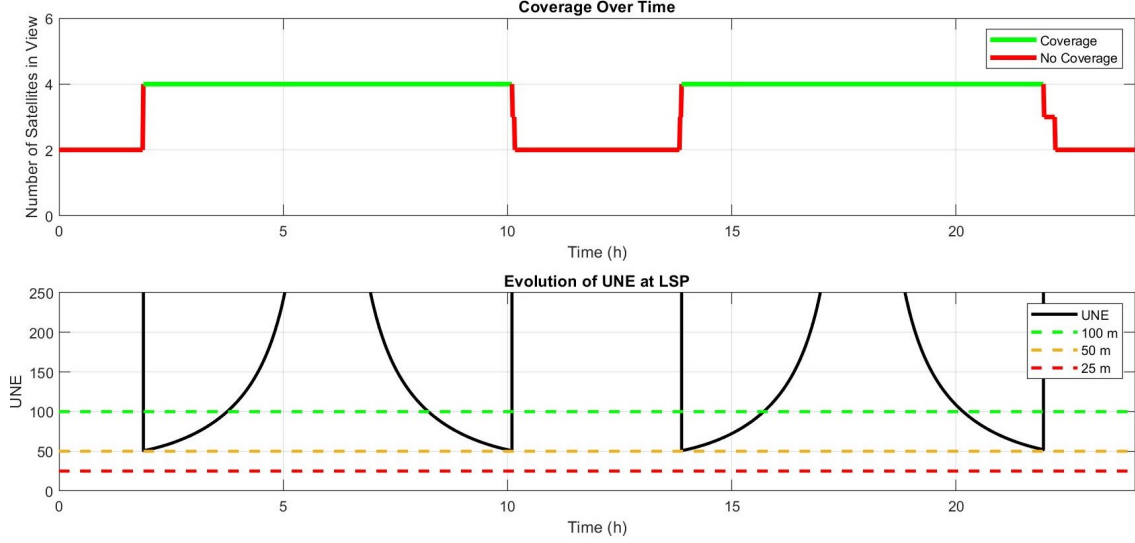
Fig. 6 For the four satellite constellation: plot of the number of satellites in view of the lunar south pole over time (Top) how the 3σ UNE changes over time at the lunar south pole (Bottom)

the 3D surface plot shown in 5a into a 2D latitude-longitude scatter plot. Similarly, each node represents one of the ground stations defined previously. This plot corroborates that the lunar south pole has the highest average number of satellites in view. Furthermore, a trend is present that the average value of satellites in view drops off as the latitude increases. As the average decreases from four satellites in view, it does not mean that there are never four satellites in view simultaneously. Many higher latitude locations are still able to obtain a position fix for at least some period of the constellation propagation despite their low averages. It is clear however, that lower latitudes are favored, which is the goal of this design.

A useful output from post processing is the coverage over time plot shown in the top of Figure 6. For the four satellite constellation, it is shown that the lunar south pole remains in coverage of the cislunar PNT system for the majority of the 24 hour propagation. The geometry of the constellation, having two satellites in mirrored orbits with a true anomaly separation of 180 degrees, results in a regular switch between four to two satellites in view. To better understand the performance implications, the PDOP for each time step of the propagation is multiplied by the total UERE displayed in Table 2. The resulting UNE over time plot for the lunar south pole is displayed as the bottom plot in Figure 6. This plot also features thresholds for desirable UNE values. This constellation results in a minimum UNE of 50 m, which occurs just as four satellites come into and leave from view. This makes sense as when two satellites become visible or no longer visible, the geometrical layout of all satellites will be the most diverse, thus reaching the lowest PDOP value. Furthermore, the absence of a UNE measurement at a time step represents a period where there are not enough satellites in view to make a measurement, which aligns with the coverage over time plot. It is noted that UNE can only achieve a lower bound that matches the value of the UERE as PDOP can only be reduced to a minimum value of 1. Therefore, achieving a low PDOP is an attainable goal for designing a constellation, but overall performance will be limited by how much the UERE can be minimized.

As seen in Table 6, the constellation spends a majority of the propagation period providing coverage to the lunar

Metric	Hours
Total Coverage Time	16.31
Max Continuous Coverage	8.23
Total Gap Time	7.69
Max Continuous Gap	3.76

Table 6 Periods of coverage and gap for the four satellite constellation

9

south pole. However, there are large gap periods that occur, which might place a constraint on any user that does not have a high fidelity IMU to use for navigation in the absence of coverage. These results are expected for an early stage constellation with the minimum number of satellites possible, and it is expected that gap times will decrease as additional satellites are added.

B. Eight Satellite Constellation

The eight satellite constellation sits at the edge of what may be considered a minimal architecture. Due to its larger constellation size, all eight satellites may be implemented at once, or there might be a two stage process of implementation. If it is the latter case, then an eight satellite constellation will be considered a later implementation of the first stage of a cislunar PNT system. The constellation being examined is one proposed by Murata Et al. [11], and the defining elements of the constellation are displayed in Table 7.

Satellite	a	e	i	Ω	ω	ν_o
1	6541.4	0.60	56.2	0	90	0
2	6541.4	0.60	56.2	0	90	90
3	6541.4	0.60	56.2	0	90	180
4	6541.4	0.60	56.2	0	90	270
5	6541.4	0.60	56.2	180	90	45
6	6541.4	0.60	56.2	180	90	135
7	6541.4	0.60	56.2	180	90	225
8	6541.4	0.60	56.2	180	90	315

Table 7   Orbit defining elements for the eight satellite constellation

One thing to note as a geometric difference between the eight and four satellite constellations is that the semimajor axes are quite different. Those of the eight satellite constellation are smaller than the four satellite constellation by approximately 3000 km. Furthermore, the orbits of the eight satellite constellation are less elliptical with a lower inclination angle, which may provide a stronger baseline constellation for building a full scale cislunar PNT system. The reasoning is that less elliptical orbits at lower inclinations will transition a constellation from a complete focus on the lunar south pole to providing better global coverage. However, for the eight satellite case being examined, the changes in the orbit geometries are not large enough to alter the constellation focus by a large amount. Similar to the four satellite architecture, the eight satellite orbit has its satellites equally spaced within an two orbital planes by means of true anomaly. However, the two mirrored orbits do have staggered true anomalies between the two, meaning that the constellations within the two orbital planes are not exactly mirrored.

An obvious result of adding more satellites to the constellation is that the average number of satellites in view across the entire lunar surface increases. Being that the eight satellite constellation also prioritizes the lunar south pole, an effect is created that looks like the average number of satellites in view is growing outwards from the south pole. As noted previously, the plots displayed in Figures 7a and 7b have a four satellite upper limit on the color map despite potentially having higher values as there are eight total satellites. In fact, it is noted that the ground stations with a color map value of exactly four actually have a higher average number of satellites in view. However, maintaining this upper limit allows for a direct comparison to the four satellite architecture in which a large performance increases in this metric is seen.

The effect of the staggered true anomalies of the eight satellite constellation is easily seen in the coverage over time plot shown in Figure 8. The transition from a maximum of eight satellites in view to a minimum of three (not including the single time step of only two) occurs in a step like fashion. Intuitively, the eight satellite constellation provides south pole coverage for a larger portion of the total propagation time. However, only for brief periods of time does the lunar south pole have all eight satellites in view. Looking at the evolution of UNE plot also shown in Figure 8, it can be seen that this architecture has an overall better performance by decreasing UNE. The larger number of satellites allows for there to be fewer periods without coverage. It is noted, however, that the minimum UNE experienced at the south pole for the eight satellite configuration is higher than that of the four satellite configuration. This indicates that the geometry of the eight satellite constellation may not be completely optimized for performance, which leaves room for improvement.
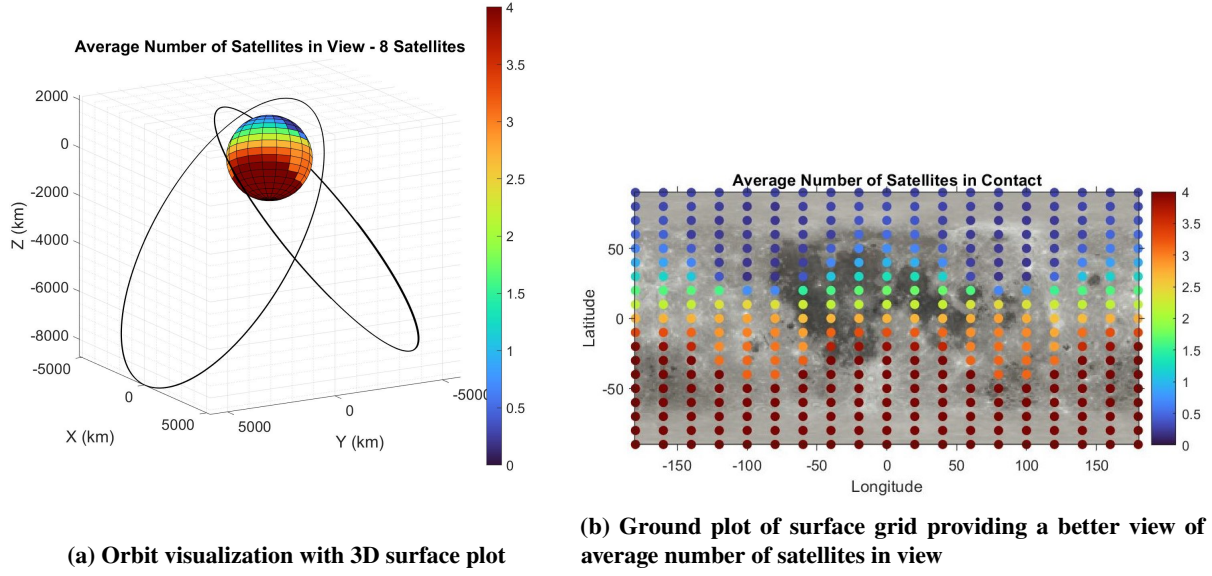
(a) Orbit visualization with 3D surface plot

(b) Ground plot of surface grid providing a better view of average number of satellites in view

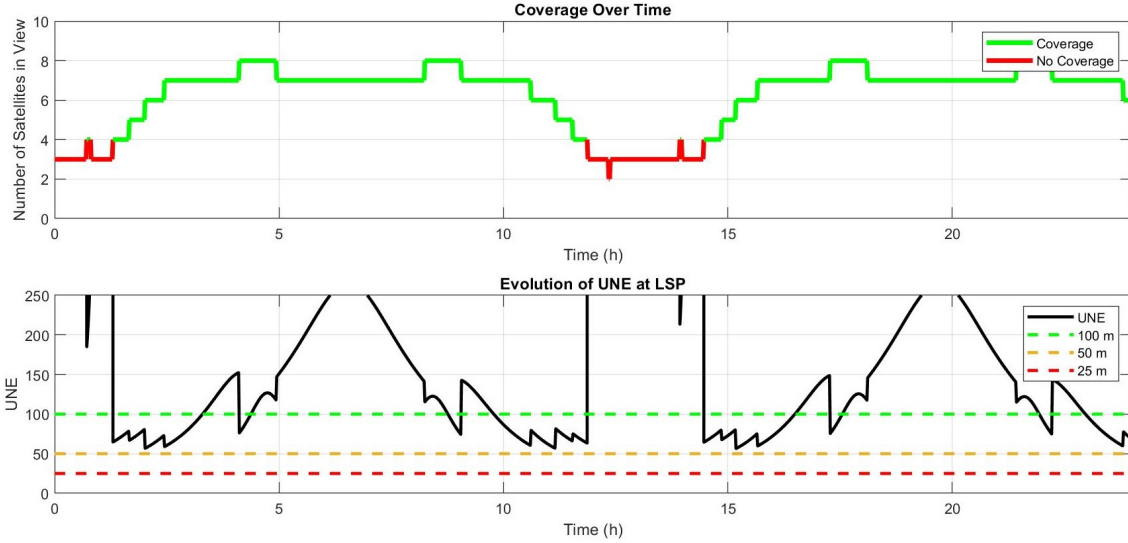**Fig. 7   Global performance visualization of the eight satellite constellation**

Fig. 8   For the eight satellite constellation: plot of the number of satellites in view of the lunar south pole over time (Top) how the 3σ UNE changes over time at the lunar south pole (Bottom)

As expected, the total coverage time for the eight satellite constellation is larger than that of of the four satellite constellation, as shown in Table 8. The maximum continuous gap time has also decreased, but it would be preferable to decrease this metric to zero, which should be possible for a eight satellite configuration. Nonetheless, any decrease in the continuous gap time reduces the strain on users to maintain an accurate PNT estimate through the use of IMUs. It is also noted that having coverage available does not necessarily mean that a useful PNT estimate can be received if the estimate contains a large amount of UNE. Therefore, maximizing coverage while minimizing UNE should be the major goal of early constellations.

Metric	Hours
Total Coverage Time	20.27
Max Continuous Coverage	10.58
Total Gap Time	3.73
Max Continuous Gap	2.05

Table 8   Periods of coverage and gap for the eight satellite constellation

VII. Novel Constellations

In order to gauge the performance of the constellations seen in literature, novel constellations are designed and examined through the modeling process. These constellations will be influenced from literature, but they will exhibit some type of alteration. The novel constellations are intended to provide better performance than those already seen, but it is important to note that these constellations are not yet optimized and merely altered for performance in an intuitive manner.

A. Six Satellite Constellation

As a middle ground between the four and eight satellite constellation seen previously, a six satellite constellation will be examined. A three satellite constellation in a single EFLO focusing on lunar south pole coverage explored by T. Ely and E. Lieb will be utilized as a base constellation [12]. The orbital elements are displayed in Table 9, and the first three rows represent the three satellites of the original constellation. The final three rows denotes the mirror of the original orbit, which was added to create the six satellite constellation. Something to note is that the eccentricity and inclination of this constellation matches those of the eight satellite constellation. The semimajor axes of the two different constellations are also similar. This is an interesting observation as it indicates that preliminary findings seem to converge on these values for being optimal for viewing the south pole within an EFLO. The true anomalies of the six satellite constellation is a major distinguisher between the current and previous constellations. Here, the satellites are not equally spaced at the starting point; instead, they are spaced in a way that optimizes south pole coverage. The spacing of satellites in an orbit is a major factor when influencing both coverage and PDOP, and it is explored in greater detail in a later section.

Satellite	a	e	i	Ω	ω	ν_o
1	6541.4	0.60	56.2	0	90	0
2	6543.98	0.60	56.2	0	90	160.15
3	6537.92	0.60	56.2	0	90	199.85
4	6541.4	0.60	56.2	180	90	0
5	6543.98	0.60	56.2	180	90	160.15
6	6537.92	0.60	56.2	180	90	199.85

Table 9   Orbit defining elements for the six satellite constellation

Figure 9a displays the 3D surface plot and orbits of the six satellite constellation. As noted previously, the similar orbit defining parameters of this constellation results in the visualization appearing to be very similar to that of the eight satellite constellation. As expected, the average number of satellites in view is greatest at lower latitudes and slowly decreases as the latitude increases. The performance in terms of average number of satellite in view sits between the four and eight satellite constellation.

More interesting results are seen in Figure 10. At the lunar south pole, the number of satellites in view over time fluctuates between four and six only, meaning that there is no drop in coverage. Based on this metric alone, it would appear that this constellation outperforms the eight satellite constellation despite having fewer total satellites. However, examining the bottom plot in Figure 10, it is seen that performance in terms of UNE may not be better. Even though there is continuous coverage, the UNE plot for the six satellite constellation displays many periods of time where the UNE is poor. In this case, the periods in which there appears to be no UNE measurement available actually indicates an
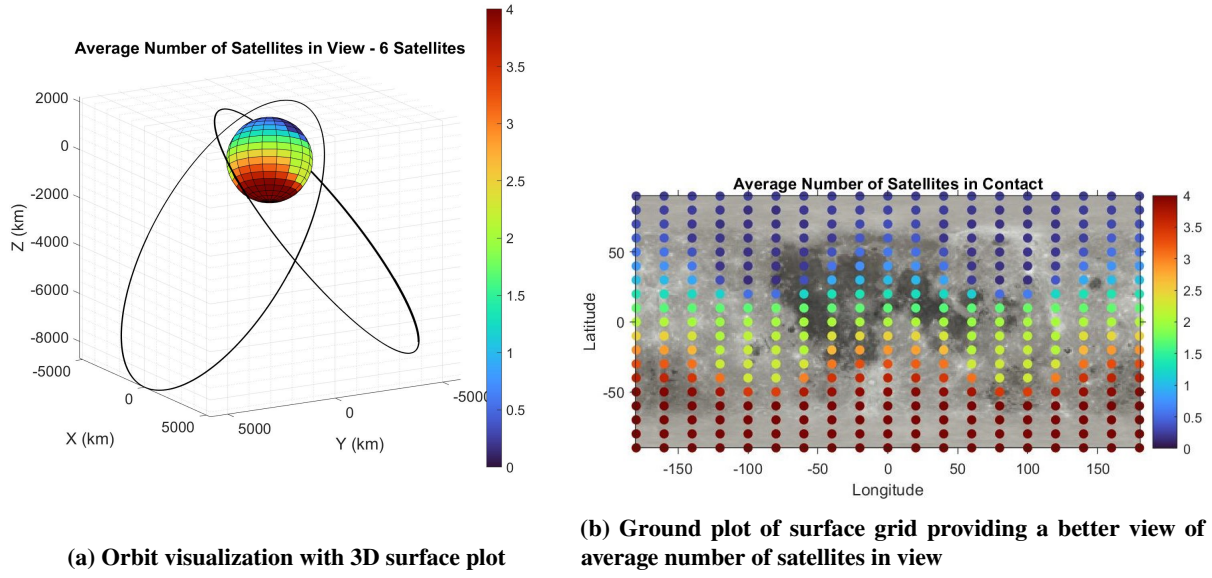
(a) Orbit visualization with 3D surface plot

(b) Ground plot of surface grid providing a better view of average number of satellites in view

Fig. 9 Global performance of the six satellite constellation

uncertainty measurement that is greater than 250 m. This result exemplifies a trade off between coverage and UNE, in which it is shown that better coverage does not necessarily imply better performance in terms of UNE. However, both can be optimized as will be seen later.

Table 10 displays the metrics relating to coverage and gap times, in which it is already known that this constellation does not experience a gap in coverage. However, the time periods in which the UNE is greater than 250 m might not prove to be useful for use cases that require greater precision, thus creating a gap time in what may be considered useful coverage.
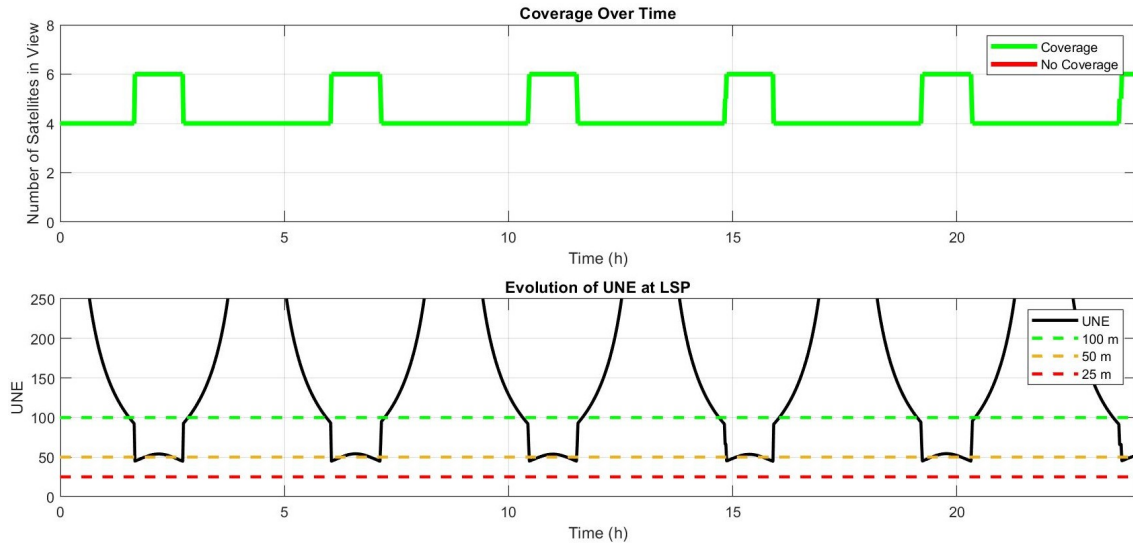

Fig. 10 For the 6 satellite constellation: plot of the number of satellites in view of the lunar south pole over time (Top) how the 3σ UNE changes over time at the lunar south pole (Bottom)

13

Metric	Hours
Total Coverage Time	24.00
Max Continuous Coverage	24.00
Total Gap Time	0
Max Continuous Gap	0

Table 10   Periods of coverage and gap for the six satellite constellation

B. Five Satellite Constellation

To explore more than just EFLOs, a constellation with a Near Rectilinear Halo Orbit (NRHO) is examined. Similar to EFLOs, NRHOs exhibit stable characteristics, meaning that their station keeping costs to maintain their orbit is small. Furthermore, NRHOs exhibit long orbit periods and large semimajor axes as they utilize the three body effects within the Earth-Moon system. Currently, NRHOs are being studied by NASA and other partners to in order to verify their stability. One such mission, CAPSTONE, is currently utilizing the NRHO selected to be used for the Lunar Gateway mission to gather more data on its characteristics [13]. For this study, a five satellite constellation will be examined using the four satellite constellation from literature that was previously modeled [10] as a base along with the addition of an NRHO. The NRHO will be modeled to replicate the trajectory of the CAPSTONE and Lunar Gateway missions. The complete set of constellation defining parameters are displayed in Table 11.

Satellite	a	e	i	Ω	ω	v_o
1	9750.5	0.70	63.50	0	90	0
2	9750.5	0.70	63.50	0	90	180
3	9750.5	0.70	63.50	180	90	0
4	9750.5	0.70	63.50	180	90	180
5	36500	0.9178	93	90	90	180

Table 11   Orbit defining elements for the five satellite constellation

As mentioned, a characteristic of an NRHO is a long orbit period. For this study, the NRHO was initialized such that it remains in view of the lunar south pole for the entire constellation propagation. As seen in Figures 11a and 11b, this results in a direct enhanced performance over the four satellite case in terms of average number of satellites in view as there is always an additional satellite above the south pole. Besides only the south pole, this also increases the average number of satellites in view for lower latitude ground stations, allowing for more user PNT estimates. It is also important to note that there will be periods of time in which the NRHO satellite is not in view of the south pole, resulting in identical coverage as that seen with the four satellite constellation. However, due to the large apoapsis of the NRHO being placed over the south pole, the satellite will spend the majority of its time in view of the south pole. Something to be examined in the future is the differing signal requirements between a satellite in an NRHO and an EFLO. The large apoapsis of an NRHO may require that the PNT satellite utilize a stronger or different signal, which can complicate the PNT architecture.

The coverage over time for the five satellite constellation, shown in the top of Figure 12, displays a shape that is identical to that of the four satellite constellation, but it is shifted upwards by one. As the constellation now alternates between three and five satellites being in view, there is not a substantial increase in total coverage time. The main performance increase comes with the improved UNE, shown in the bottom of Figure 12. While at least four satellites are in view, the UNE reaches a minimum value of just below 50 m and a maximum of around 125 m. A majority of the UNE measurements sit under the least strict threshold of 100 m, which is a major improvement. Besides having the additional satellite in view at all times, an explanation for this result may be that the NRHO satellite provides a constant diversification of the constellation geometry during the propagation period. In turn, the NRHO reduces the PDOP due to its geometry along with adding an additional source of measurements. In terms of average performance directly based on UNE, the five satellite constellation outperforms all constellations previously examined for the period in which the NRHO is present.
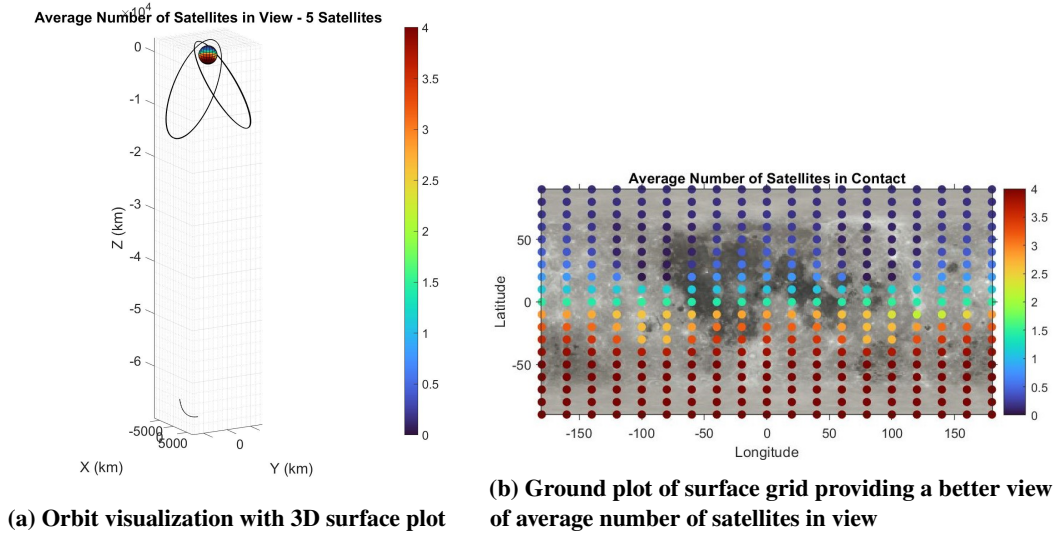
14

(a) Orbit visualization with 3D surface plot

(b) Ground plot of surface grid providing a better view of average number of satellites in view

Fig. 11   Global performance of the five satellite constellation
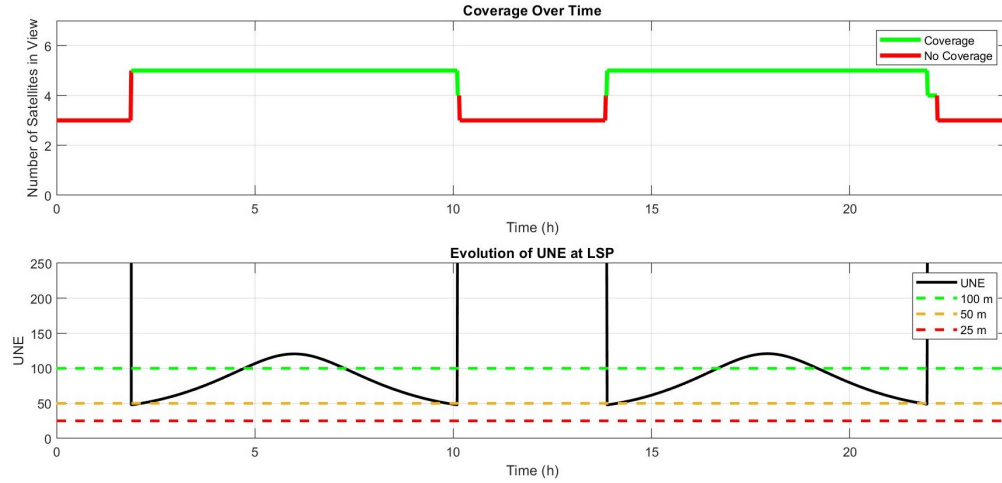

Fig. 12   For the 5 satellite constellation: plot of the number of satellites in view of the lunar south pole over time (Top) how the 3σ UNE changes over time at the lunar south pole (Bottom)

As mentioned, despite the major improvement of UNE, the coverage between the four and five satellite constellation cases remain to be very similar, in which the metrics for the five satellite constellation can be seen in Table 12. This once again shows that improvement in either coverage or UNE does not guarantee improvement of both. Of course, allowing for complete coverage will result in PNT measurements to always be made, but those measurements may not meet the needs of users. These two metrics should be thought of as being linked, but not in a straightforward linear fashion.

Metric	Hours
Total Coverage Time	16.64
Max Continuous Coverage	8.36
Total Gap Time	7.36
Max Continuous Gap	3.68

Table 12   Periods of coverage and gap for the five satellite constellation

VIII. Optimization for Minimal Satellite Constellations

There is ample room for increasing constellation performance in terms of both coverage and UNE while focusing on the lunar south pole. As shown in Section VII, improvements can quickly be made over constellations studied in literature by making architectural changes. This poses a pressing question: how much more performance increase can be achieved for a minimal constellation? To address this, an optimization process is employed in order to systematically find the most desirable constellation orientations, which is defined in this study as exhibiting a low UNE and high proportion of time spent in coverage. In order to do this, the ephemerides of a propagated satellite constellation are loaded into MATLAB. The ephemerides for each time step are used to calculate the UNE at that instance, in which all time steps are combined in an order specified by the initial true anomalies that are input to the function. A MATLAB based optimizer iterates on the initial true anomalies of the satellites as parameters to optimize in order to produce a new configuration with better performance.

It is important to note here that the optimization process will not reduce the proportion of time a single satellite will spend in view of the south pole, but it will affect the coverage at the south pole. The orbit itself defines the proportion of time the satellite is in view, and the optimization process will leave the orbit geometry unchanged. However, spacing within an orbit will alter the number of satellites in view of the lunar south pole at any given time. The optimization in this section does not optimize for maximizing coverage; however, due to the fact that there must be coverage in order to obtain a position fix, coverage will automatically be accounted for. This is further made possible by utilizing a cost function that induces a penalty when a UNE measurement is not available, which is synonymous with not having coverage. To do this, the UNE variable in Equation 7, which is the objective function, is given some high value when coverage is not available for that time step. The penalty used in this study is a UNE value of 2000. Furthermore, the objective function also has the proportion of time spent in coverage squared in the denominator. This forces the optimization to value solutions that have a consistently lower UNE with higher coverage rather than those with instances of much lower UNE that skew the average. In Equation 7, N is the number of total time steps in the propagation and i is the current iteration.

$$min(\nu_o) \quad \frac{\sum_{i=1}^{N} UNE}{N * (prop\ of\ time\ in\ coverage)^2} \tag{7}$$

The optimization method used in MATLAB is a Nelder-Mead simplex method, which is a direct search method. It operates without needing information regarding the first or second derivative of the objective function, which is valuable to this study as approximating the derivative through means of a finite difference scheme with a large number of time steps would induce a major computational cost. The Nelder-Mead method works by evaluating the objective function at selected locations, which are variations in the starting true anomalies, in which it determines which of the locations evaluated are the most desirable. It then searches in the direction of decreasing objective function value in order to eventually find a minimum.

The UNE optimization process is applied to the six and eight satellite constellations previously examined in this study. It was found that optimizing using this method for a constellation with less than six satellites was largely unproductive due to the constellation containing the minimum number of satellites necessary to perform the PDOP calculation. Small changes in the initial true anomalies of satellites would drastically alter the coverage time at the lunar south pole, which resulted in offsetting any performance enhancements achieved through PDOP. However, interesting results were obtained for both the six and eight satellite cases utilizing the orbital parameters displayed in Tables 9 and 7, respectively.

A. Six Satellite Optimization

It is first noted that due to the problem being very large and highly configurable, there is no clear gradient to the objective function. There are many local minimums as there are an infinite number of combinations to orient the satellites within their orbits. For the six satellite case, if starting true anomalies are limited to being integers, then there are 360^6 combinations of satellite spacing that can be used as an initial guess for the optimization. It was found that small changes in the initial guess affect the results greatly, which is a sign that the optimization problem is not well defined. To counteract this, a series of optimizations were systematically run using a wide variety of starting locations. This is mentioned in order to give a view of the true magnitude of an optimization problem this size.

Table 13 displays the possible initial guesses for each satellite, in which the algorithm ran an optimization with each possible combination, which resulted in running the optimization 1296 times. From each combination of initial guesses, the minimized objective function, the value of Equation 7, was calculated along with the optimal true anomalies to

Starting Guesses for Each Satellite	
Sat 1	[0 45 90 135]
Sat 2	[135 180 225]
Sat 3	[225 270 315]
Sat 4	[0 45 90 135]
Sat 5	[135 180 225]
Sat 6	[225 270 315]

Table 13   Every possible initial guess used for each satellite in the six satellite constellation

Case	TA_1	TA_2	TA_3	TA_4	TA_5	TA_6	Fun Val	Avg PDOP
1	0.00	178.64	223.41	79.99	186.32	211.72	195.84	10.86
2	170.14	148.04	257.22	-.01	128.47	184.67	199.18	10.78
3	96.88	186.96	271.75	134.49	201.04	226.31	199.27	9.19
4	111.94	190.23	215.71	44.83	180.89	231.62	200.28	8.65
Original	0.00	160.15	199.85	0.00	160.15	199.85	937.28	28.42

Table 14   Optimal starting true anomalies for the satellites in the six satellite constellation

produce that minimized value. It is noted that no two set of initial guesses yielded the same optimized result, which further shows the extreme nonlinearity of this problem. After running the optimization, the best performers are displayed in Table 14. It can be seen that Case 1 performs the best when minimizing the objective function, but Case 4 performs the best in terms of average PDOP. Here, PDOP is calculated as the average PDOP while coverage is available and it does not take into account the penalty when there is no coverage. Due to this, Case 1 performs better in terms of the objective function, which does apply the no coverage penalty, as it has a slightly higher proportion south pole coverage than Case 4. Therefore, Case 1 has periods of coverage with a higher PDOP during periods that Case 4 has no coverage, which does not negatively affect average PDOP metric displayed in Table 14. Overall, all cases outperform the original configuration, whose function value and average PDOP are displayed in the bottom row of the table.

The plot of UNE over time at the lunar south pole for Case 1 is displayed at the bottom of Figure 13, with the same plot for the original six satellite constellation at the top. It can directly be seen that the optimized configuration provides a larger amount of time with a lower UNE. However, the strange characteristic shape of the plot with sharp dips and changes in performance may be undesirable to users as opposed to a more predictable pattern. A better performing solution with a lower average UNE may exist despite not being found by the optimizer. Statistical comparison metrics are displayed in Table 15. The original case outperforms the optimized case for the proportion of coverage; however, it does so by a negligible small margin. The optimized case exhibits a smaller active mean UNE, where active indicates that the mean was taken using time steps in which coverage was available. An interesting note is that the optimized case has a larger minimum UNE than the original case, which may be attributed to the fact that the optimized case focuses on minimizing the objective function that is influenced by the average UNE. Further affects of optimizing on the average UNE is that variance of the optimized case is much smaller than that of the original case. Variance indicates the variation of measurements from the mean value. Therefore, a smaller variance is desired due to the fact that it means that UNE measurements for each time step tend to remain close to the mean without major fluctuations. Overall, the optimized six satellite configuration is shown to be more desirable than the original.

Case	Coverage Proportion	Active UNE Mean	Active UNE Var	Min UNE	Max UNE
1	0.999	146.61	1630.30	53.84	960.31
Original	1.00	223.89	5863.72	44.66	1487.97

Table 15   Statistical metrics for 3σ UNE of the six satellite constellation cases
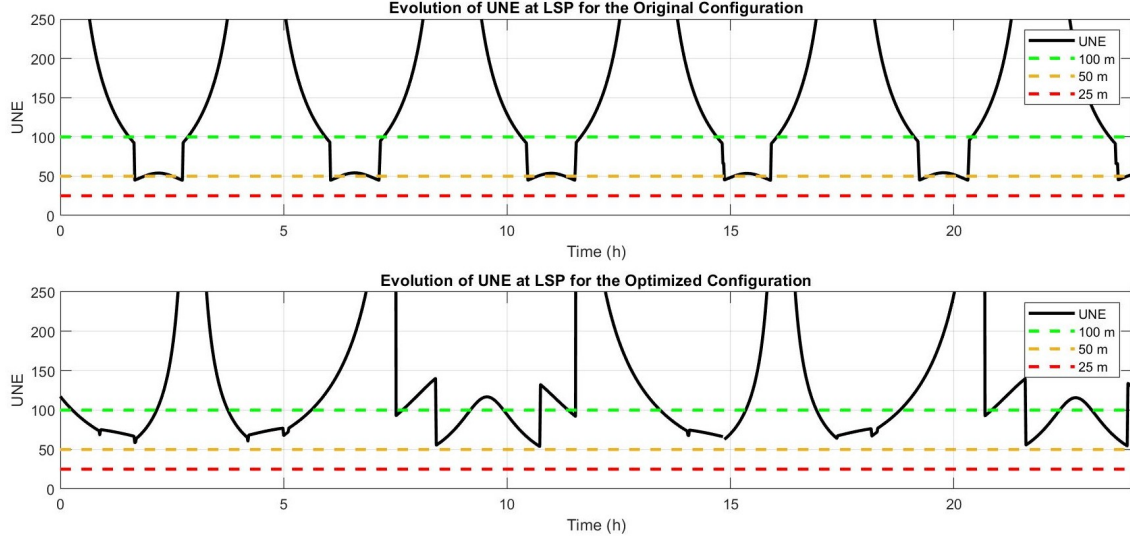
Fig. 13   The 3σ **UNE over time for the lunar south pole for the original six satellite case (Top) and the optimized Case 1 (Bottom)**

B. Eight Satellite Optimization

The same optimization process was applied to the eight satellite constellation and the initial conditions for optimization are displayed in Table 16. Due to the additional two satellites, optimizing using this method requires 6561 individual optimizations, which is a considerable computational increase over the six satellite case. However, it is once again noted that no two different initial guesses to initialize the optimization resulted in the algorithm producing identical results, which corroborates the importance of providing a variety of initial guesses. The best performing cases

Starting Guesses for Each Satellite	
Sat 1	[0 45 90]
Sat 2	[45 90 135]
Sat 3	[135 180 225]
Sat 4	[225 270 315]
Sat 5	[0 45 90]
Sat 6	[90 135 180]
Sat 7	[180 225 270]
Sat 6	[270 315 360]

Table 16   Every possible initial guess used for each satellite in the eight satellite constellation

are displayed in Table 17, in which it seen that like for the six satellite constellation, all optimized cases outperform the original model. Case 1 performed the best in both minimizing the objective function and having the lowest average PDOP. A major contributor to the enhanced performance of Case 1 is that the constellation allows for the lunar south pole to receive coverage at all times, which is something that the original constellation fails to do. The result of this is a decrease in both the objective function and average PDOP for the original case.

Figure 14 displays the UNE over time at the lunar south pole for the original constellation and the Case 1 optimized constellation. Drastic performance increases are observed as the UNE for the optimized configuration spends a majority of the simulation being below the 100 m threshold and never increasing above 175 m. Towards the beginning and just after the midpoint of the simulation, there appears to be abrupt spikes in the UNE, which would be smoothed over in practice through filtering or by the use of IMUs. The other sharp changes in UNE occur when a satellite either comes into or goes out of view of the lunar south pole.

18

Case	TA_1	TA_2	TA_3	TA_4	TA_5	TA_6	TA_7	TA_8	Fun Val	Avg PDOP
1	43.69	183.34	152.58	216.87	42.90	152.22	182.82	217.22	76.11	3.53
2	39.51	151.30	183.05	217.49	43.74	216.50	182.73	152.23	76.15	3.54
3	-0.01	148.61	179.93	212.49	-0.01	147.51	212.42	179.71	76.17	3.64
4	43.87	147.29	181.94	212.14	0.01	151.47	179.74	216.24	77.03	3.61
Original	0	90	180	270	45	135	225	315	198.42	4.52

Table 17 Optimal starting true anomalies for the satellites in the eight satellite constellation

As mentioned, having complete coverage is a major improvement for the constellation as periods in which the original orientation has no coverage, the optimized case allows for UNE that is below the 100 m threshold. Table 18 displays other statistical metrics that help compare the optimized case with the original case, in which it is seen that the optimized case outperforms the original for all metrics. As noted when evaluating the six satellite constellation, the active UNE mean and variances do not factor in penalties applied when there is an absence in coverage. If the penalties were included, the performance metrics of the original case would be much worse than those displayed in the table. While maintaining constant coverage, the optimized case exhibits a mean UNE below 100 m and a variance much smaller than that of the original case. Furthermore, the optimized constellation reaches a minimum UNE just above 38. This is well below the intermediate threshold of 50 m, reaching a level of performance that is much better than the previously examined constellations.
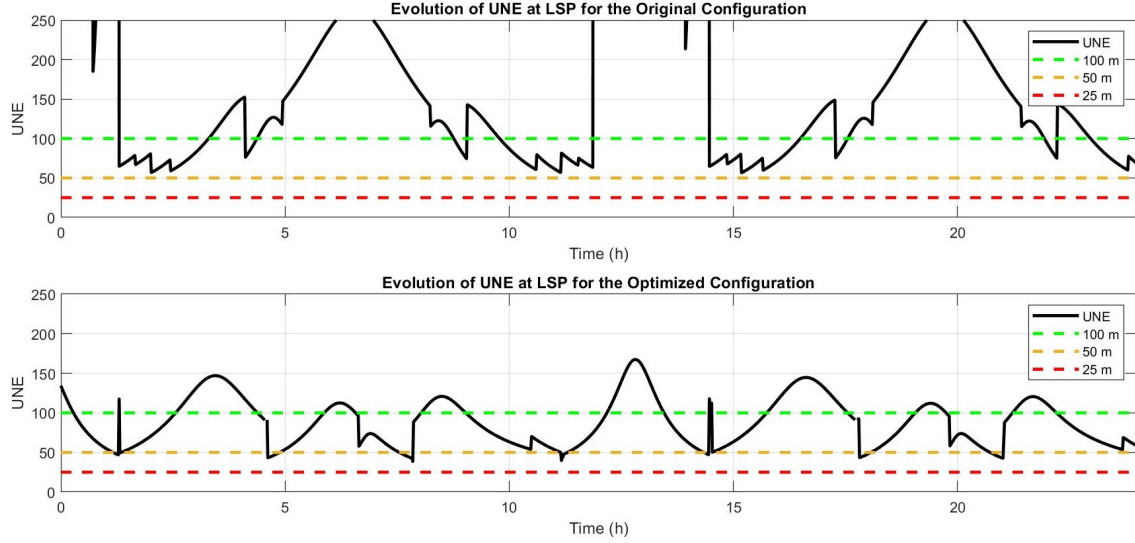

Fig. 14 The 3σ UNE over time for the lunar south pole for the original eight satellite case (Top) and the optimized Case 1 (Bottom)

Case	Coverage Proportion	Active UNE Mean	Active UNE Var	Min UNE	Max UNE
1	1.00	87.741	914.509	38.459	167.454
Original	0.845	132.965	4098.889	56.494	287.848

Table 18 Statistical metrics for 3σ UNE of the eight satellite constellation cases

IX. Conclusion

To permanently fill the increasing needs of users operating within cislunar space, a dedicated PNT system should be implemented. Viable architectures will most likely be constructed in phases similar to what was seen for GPS, meaning that there will be a near and late term implementation. The immediate focus should be on the near term PNT architecture, defined as having between four and eight satellites, in which service will be directed to locations of interest, primarily being the lunar south pole. There are an infinite number of possible near term implementations; however, by defining a standard set of performance metrics, different constellation geometries can be assessed for their efficacy and therefore be compared. System coverage, service gap time, PDOP, and UNE are metrics that are determined based on constellation and orbit geometry and allow for a first look into the performance of early PNT architectures.

A modeling process was developed using Python, GMAT, and MATLAB in order to calculate the metrics of interest for constellations studied in literature, novel constellations influenced by literature, and optimized constellations. It is found that, consistent with intuition, a higher number of PNT satellites yields better performance in terms of UNE and coverage. Furthermore, early architectures recommended by literature serve as a good starting point for constellation development but leave ample room for improvement. When adding an NRHO to the four satellite constellation, a major performance increase was observed. This indicates that other orbit types besides EFLOs would be a valuable asset in a PNT constellation. As coverage and UNE are heavily influenced by satellite orientation within an orbit, it is shown that optimizing satellite positioning will draw out increased performance for existing constellations. The best performance was achieved by the optimized eight satellite constellation, in which the minimum 3σ UNE was just above 38 m. This is a promising preliminary result as the projected requirements for total 3σ positioning error for lunar surface operations is 30 m [4]. This threshold, along with others that are more stringent, is very likely to be met by the presented constellations with the inclusion of Kalman or batch measurement filtering.

In the future, performance analysis of PNT constellations will need to be applied to other users, like low lunar orbiters, as near term operations in cislunar space will not only be limited to surface users. Furthermore, near term architectures employing more than a pair of mirrored orbits should be examined. It might be useful to construct a constellation with three or four orbits utilizing a combination of EFLOs and NRHOs. Of course, broadening constellation solutions will greatly increase the scope of the problem, but it is necessary in order to converge on the best possible solution. At a certain point, constellation optimization will provide the best orbit geometries that minimize PDOP; therefore, the next major focus should be to reduce UERE. If consistent performance is desired to be below 25 m of UNE, then the UERE needs to be significantly reduced as it currently induces the majority of uncertainty. It is noted that the UERE value utilized in this study is a worst case scenario and that actual UNE may be smaller, but it is deemed best to understand and characterize the worst case performance of the system.

Overall, this study presents the motivation for developing a cislunar PNT system along with a set of metrics that are useful for evaluating potential candidates. It is shown that applying constellations to the developed modeling process allows for a standardized comparison of performances. Finally, results demonstrate that performing optimization on the identified metrics leads to an overall performance increase to help identify the best possible early stage cislunar PNT system.

References

[1] Chang, C., Kinman, P., O'Dea, A., and Pham, T., "Doppler Tracking," , 7 2022. URL `https://deepspace.jpl.nasa.gov/dsndocs/810-005/202/202E.pdf`.

[2] Border, J., Change, C., Pham, T., and Shin, D., "Delta Differential One-way Ranging," , 2 2021. URL `https://deepspace.jpl.nasa.gov/dsndocs/810-005/210/210D.pdf`.

[3] Winternitz, L., Bamford, W., Long, A., and Hassouneh, M., "GPS Based Autonomous Navigation Study for the Lunar Gateway," , 1 2019. URL `https://ntrs.nasa.gov/api/citations/20190002311/downloads/20190002311.pdf`.

[4] Nelson, R., Brodsky, B., Oria, A., Connolly, J., Sands, O., Welch, B., Ely, T., Orr, R., and Schuchman, L., "Key Issues for Navigation and Time Dissemination in NASA's Space Exploration Program," , 2006.

[5] Small, J. L., Mann, L. M., Crenshaw, J. M., Gramling, C. J., Rosales, J. J., Winternitz, L. B., Hassouneh, M. A., Baker, D. A., Hur-Diaz, S., and Liounis, A. J., "Lunar Relay Onboard Navigation Performance and Effects on Lander Descent to Surface," 2022, pp. 587–601. https://doi.org/10.33012/2022.18221.

[6] Misra, P., and Enge, P., *Global Positioning System: Signals, Measurements and Performance*, 2nd ed., 2010.

[7] Nie, T., and Gurfil, P., "Lunar Frozen Orbits Revisited," *Celestial Mechanics and Dynamical Astronomy*, Vol. 130, 2018, p. 61. https://doi.org/10.1007/s10569-018-9858-0.

[8] Zimovan, E. M., Howell, K. C., and Davis, D. C., "Near rectilinear halo orbits and their application in cis-lunar space," *3rd IAA Conference on Dynamics and Control of Space Systems, Moscow, Russia*, Vol. 20, 2017, p. 40.

[9] Pereira, F., and Selva, D., "Analysis of Navigation Performance with Lunar GNSS Evolution," 2022, pp. 514–529. https://doi.org/10.33012/2022.18210.

[10] Bhamidipati, S., Mina, T., and Gao, G., "A Case Study Analysis for Designing a Lunar Navigation Satellite System with Time-Transfer from Earth-GPS," 2022.

[11] Murata, M., Kawano, I., and Kogure, S., "Lunar Navigation Satellite System and Positioning Accuracy Evaluation," 2022, pp. 582–586. https://doi.org/10.33012/2022.18220.

[12] Ely, T. A., and Lieb, E., "Constellations of elliptical inclined lunar orbits providing polar and global coverage," *The Journal of the Astronautical Sciences*, Vol. 54, 2006, pp. 53–67. https://doi.org/10.1007/BF03256476.

[13] Thompson, M. R., Forsman, A., Chikine, S., Peters, B. C., Ely, T., Sorensen, D., Parker, J., and Cheetham, B., "Cislunar Navigation Technology Demonstrations on the CAPSTONE Mission," 2022, pp. 471–484. https://doi.org/10.33012/2022.18208.